# Binding of manganese(II) to a tertiary stabilized hammerhead ribozyme as studied by electron paramagnetic resonance spectroscopy

NATALIA KISSELEVA,[1] ANASTASIA KHVOROVA,[2] ERIC WESTHOF,[3] and OLAV SCHIEMANN[1]

[1]Institute of Physical and Theoretical Chemistry, Center of Biomolecular Magnetic Resonance, Johann Wolfgang Goethe-University, Marie-Curie-Strasse 11, 60439 Frankfurt am Main, Germany
[2]Dharmacon Research, Inc., Lafayette, Colorado, 80026 USA
[3]Institut de Biologie Moléculaire et Cellulaire, UPR9002 du CNRS, Université Louis Pasteur, 15 rue René Descartes F-67084, Strasbourg Cedex, France

## ABSTRACT

**Electron paramagnetic resonance (EPR) spectroscopy is used to study the binding of $Mn^{II}$ ions to a tertiary stabilized hammerhead ribozyme (tsHHRz) and to compare it with the binding to the minimal hammerhead ribozyme (mHHRz). Continuous wave EPR measurements show that the tsHHRz possesses a single high-affinity $Mn^{II}$ binding site with a $K_D$ of ≤10 nM at an NaCl concentration of 0.1 M. This dissociation constant is at least two orders of magnitude smaller than the $K_D$ determined previously for the single high-affinity $Mn^{II}$ site in the mHHRz. In addition, whereas the high-affinity $Mn^{II}$ is displaced from the mHHRz upon binding of the aminoglycoside antibiotic neomycin B, it is not from the tsHHRz. Despite these pronounced differences in binding, a comparison between the electron spin echo envelope modulation and hyperfine sublevel correlation spectra of the minimal and tertiary stabilized HHRz demonstrates that the structure of both binding sites is very similar. This suggests that the $Mn^{II}$ is located in both ribozymes between the bases A9 and G10.1 of the sheared G · A tandem base pair, as shown previously and in detail for the mHHRz. Thus, the much stronger $Mn^{II}$ binding in the tsHHRz is attributed to the interaction between the two external loops, which locks in the RNA fold, trapping the $Mn^{II}$ in the tightly bound conformation, whereas the absence of long-range loop–loop interactions in the mHHRz leads to more dynamical and open conformations, decreasing $Mn^{II}$ binding.**

**Keywords: Hammerhead ribozyme; EPR; manganese; antibiotic; RNA; ESEEM**

## INTRODUCTION

The hammerhead ribozyme (HHRz) is a naturally occurring ribozyme that can site-specifically cleave the phosphodiester backbone of RNA (Gesteland et al. 1999). The minimal hammerhead ribozyme (mHHRz) motif consists of three helices connected by a highly conserved catalytically active core of 11 nucleotides at the three-way junction. This mHHRz can cleave RNA in the presence of high concentrations of $Mg^{II}$ (>5 mM) but is inactive under physiological salt concentrations. Recently it was shown that the ribozyme becomes catalytically active at salt concentrations as encountered in vivo (0.1–0.3 mM) by including nonconserved sequence elements outside of the catalytic core (Fig. 1; De la Pena et al. 2003; Khvorova et al. 2003). In some sequences, these sequence elements lead to the formation of two interacting loops at the ends of helices I and II, as demonstrated by sequence alignments and molecular modeling (Khvorova et al. 2003) as well as fluorescence energy transfer (FRET) measurements (Penedo et al. 2004). These additional long-range interactions stabilize the tertiary fold of the RNA and decrease its requirement for divalent metal ions. Here we want to investigate whether the presence of these loops changes the affinity, position, and structure of the metal(II) ion binding sites in comparison to the mHHRz using electron paramagnetic resonance (EPR) spectroscopy.

EPR spectroscopy is a technique by which the binding of paramagnetic metal(II) ions to RNA can be probed in a direct way. Especially modern pulsed EPR methods like electron spin echo envelope modulation (ESEEM) (Dikanov and Tsvetkov 1992) and hyperfine sublevel correlation experiments (HYSCORE) (Benetis et al. 2002) allow the gathering of information about the type and structure of

**Reprint requests to:** Olav Schiemann, Institute of Physical and Theoretical Chemistry, Center of Biomolecular Magnetic Resonance, Johann Wolfgang Goethe-University, Marie-Curie-Strasse 11, 60439 Frankfurt am Main, Germany; e-mail: o.schiemann@epr.uni-frankfurt.de; fax: 49(0)69-79829404.

Article and publication are at http://www.rnajournal.org/cgi/doi/10.1261/rna.7127105.

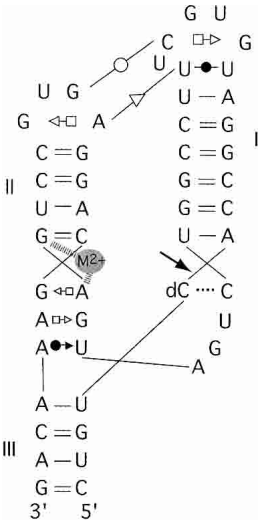


**FIGURE 1.** Secondary structure of the tsHHRz. The cleavage site is indicated by an arrow; the interactions between the nonconserved sequence elements outside of the catalytic core are depicted with the potential tertiary contacts indicated (Khvorova et al. 2003). The gray ball denotes the binding site of $Mn^{II}$ connecting A9 and G10.

surrounding ligands of metal centers, whereas pulsed electron double resonance (Schiemann et al. 2004) could be used to localize these metal ions in the global context of the RNA fold. However, to be able to apply these methods, the naturally occurring diamagnetic $Mg^{II}$ has to be substituted by the paramagnetic $Mn^{II}$ (S = 5/2, I = 5/2) as done in previous studies on the mHHRz (Horton et al. 1998; Schiemann et al. 2003). The catalytic activity of RNA is usually reduced in the presence of $Mn^{II}$ despite the fact that both metal ions have some similar physical and chemical properties (Feig 2000). However, $Mn^{II}$ occupies in the crystal structures of the mHHRz the same binding pocket and adopts the same structure as the $Mg^{II}$ ion (Pley et al. 1994; Scott et al. 1996).

## RESULTS AND DISCUSSION

### Quantification of $Mn^{II}$ binding sites

Manganese(II) ions in an aqueous solution give at room temperature a continuous wave (cw) EPR signal of six lines due to the coupling of the electron spin S of 5/2 to the $^{55}Mn$ nuclear spin I of 5/2. If, however, the manganese ions form a large asymmetric complex, for example, with a protein or RNA, the relaxation times increase and the lines broaden significantly or may even become undetectable (Misra 1996). This effect can be used, as in the case of the mHHRz (Horton et al. 1998; Schiemann et al. 2003), to quantify the $Mn^{II}$ sites in the tertiary stabilized hammerhead ribozyme (tsHHRz) by monitoring the manganese cw EPR signal intensity while titrating $Mn^{II}$ into the ribozyme solution (pH = 7). The graphical representations of three such titrations are shown in Figure 2A. One titration was done with a sample containing 0.1 mM tsHHRz and 1 M NaCl and the second with a sample also containing 0.1 mM tsHHRz but only 0.1 M NaCl in the phosphate buffer solution. In the third case, $Mn^{II}$ was titrated into a phosphate buffer solution containing 1 M NaCl but no ribozyme for the sake of comparison.

From the titration of the tsHHRz in the presence of 1 M NaCl, the binding isotherm in Figure 3A was constructed as explained in Materials and Methods. The fit of the experimental data with Equation 1 shows that the tsHHRz possesses in the presence of 1 M NaCl three cooperative $Mn^{II}$ binding sites with $K_D$s of 166 μM ± 18 μM. Reducing the NaCl concentration to 0.1 M results in the occupation of only a single high-affinity $Mn^{II}$ binding site. As can be nicely seen in the inset in Figure 2A, the EPR signal does not increase up to a $Mn^{II}$/tsHHRz ratio of 1:1, demonstrating that all added manganese ions are, up to this ratio, tightly bound to the RNA. Due to the obviously very strong bind-

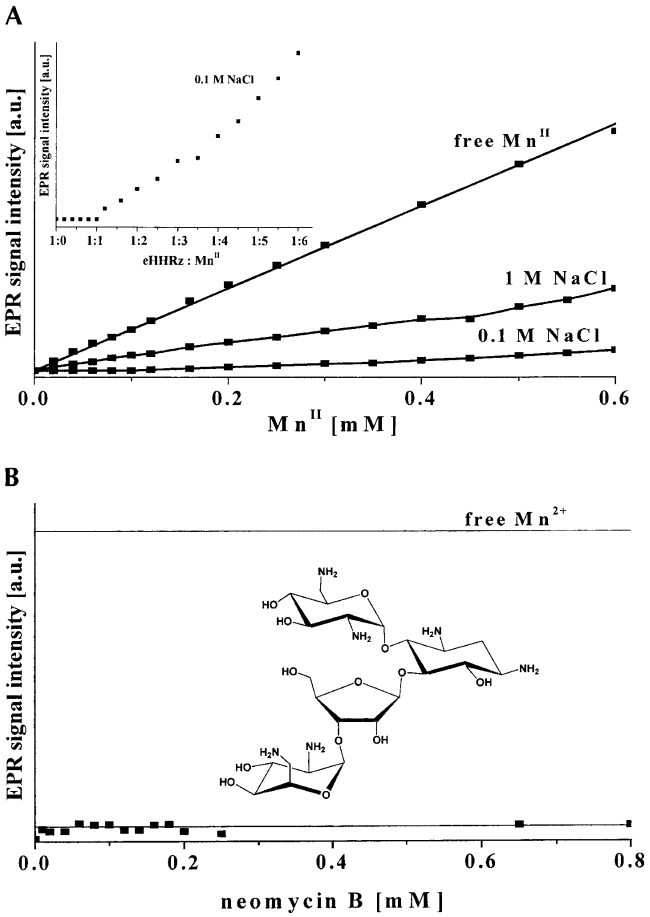


**FIGURE 2.** (*A*) $Mn^{II}$ titration curves of samples containing only buffer (free $Mn^{II}$); containing 0.1 mM ribozyme and 1 M NaCl (1 M NaCl); and containing 0.1 mM ribozyme and 0.1 M NaCl (0.1 M NaCl). The *inset* shows a plot of the $Mn^{II}$ EPR signal intensity against the ratio of ribozyme to $Mn^{II}$ in the presence of 0.1 M NaCl. (*B*) Titration of the 1:1 complex of tsHHRz/$Mn^{II}$ with neomycin B.

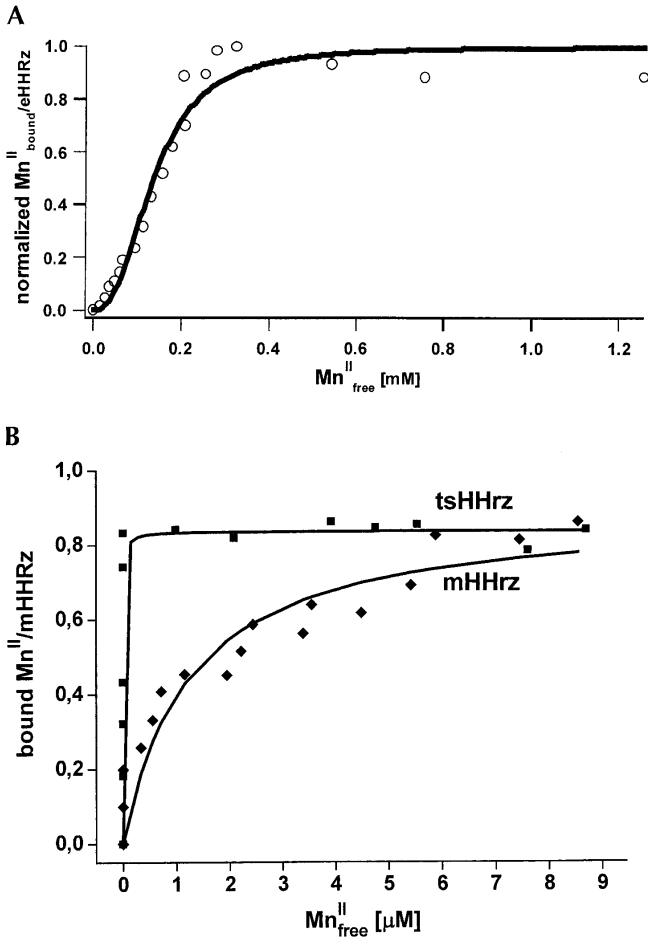


**FIGURE 3.** (*A*) Binding isotherm constructed from the data in Figure 2 for the tsHHRz in the presence of 1 M NaCl ($n = 3.1 \pm 0.3$, $K_D = 166 \pm 18$ μM). (*B*) Binding isotherms constructed for the mHHRz in the presence of 1 M NaCl ($n = 1.0 \pm 0.2$, $K_D = 4.4 \pm 0.5$ μM) and for the tsHHRz in the presence of 0.1 M NaCl ($n_1 = 1.0 \pm 0.4$, $K_{D,1} \leq 10$ nmol and $n_2 = 16 \pm 4$, $K_{D,2} = 129$ μM ± 31 μM), both for ribozyme concentrations of 1 μM. The circles and squares in the graphs are the experimental points and the lines correspond to the respective fits using Equation 1 (*A*) and Equation 2 (*B*).

ing, the titrations were repeated for the mHHRz and the tsHHRz at ribozyme concentrations of 1 μM to reveal differences in $K_D$. It can immediately be seen from Figure 3B that the binding of $Mn^{II}$ to the tsHHRz is much stronger than to the mHHRz. Constructing for both the binding isotherms and fitting them with Equation 2 yielded for the mHHRz a single binding site with a $K_D$ of 4 μM. This dissociation constant of 4 μM does not change upon decreasing the NaCl concentration from 1 to 0.1 M, whereas the amount of $Mn^{II}$ binding sites increases from 1 to 4 (Horton et al. 1998; Schiemann et al. 2003). The fit of the binding isotherm of the tsHHRz yields an upper limit for the dissociation constant of 10 nM (best fit 1 nM) and $16 \pm 4$ low-affinity sites with $K_D$s of 129 μM ± 31 μM (Fig. 3B). This shows that the tsHHRz possesses, like the mHHRz, a single high-affinity $Mn^{II}$ binding site but that the binding in this site is at least two orders of magnitude stronger. Intriguingly, this parallels the observation that the tsHHRz is catalytically active at physiological salt concentrations whereas the mHHRz is not (Khvorova et al. 2003; Penedo et al. 2004). The increase in $Mn^{II}$ binding sites upon lowering the NaCl concentration is attributed to the decrease of the ionic strength of the buffer. In other words, at high ionic strength, the negatively charged parts of the ribozyme are screened by the sodium ions and $Mn^{II}$ has to compete with the high amount of monovalent ions for the binding pockets.

## Binding of neomycin B

The extremely strong binding of the single $Mn^{II}$ prompted us to investigate whether the antibiotic neomycin B is capable of displacing it from the ribozyme, as was found for the single high-affinity $Mn^{II}$ in the mHHRz (Schiemann et al. 2003). Figure 2B shows the titration of the tsHHRz/$Mn^{II}$ complex with neomycin B in the presence of 0.1 M NaCl (single nM binding site occupied by a single $Mn^{II}$). If neomycin B would bind to the tertiary stabilized ribozyme and displace the manganese from its binding site into solution, the EPR signal intensity would increase with increasing neomycin B concentration. However, it is observed that the EPR signal intensity does not increase but stays close to zero, which indicates instead that the manganese ion is not displaced from the ribozyme. This is supported by the observation that the dissociation constant for neomycin B is already in the case of the mHHRz only slightly smaller than that for $Mn^{II}$.

One simple reason may be that neomycin B does not bind at all to the tsHHRz. Another explanation could be that neomycin B does bind to the ribozyme but with the positively charged ammonium groups in positions not capable of competing with the $Mn^{II}$ for the high-affinity binding site (Hermann and Westhof 1998). This would occur if the tsHHRz adopted a tighter global fold than the mHHRz, thereby decreasing the size of the central cavity formed by the three-way junction where the antibiotic would have to bind in order to displace the ion (Khvorova et al. 2003).

## Pulsed EPR measurements

The relaxation times of the $Mn^{II}$ center in the single high-affinity binding site are, at room temperature, too fast to detect an EPR signal. To overcome this problem and to be able to gather structural information about this site, the sample was frozen to 4.2 K. Under these conditions pulsed EPR sequences like 2D-3-pulse ESEEM and HYSCORE can be applied. The spectra of both methods are characteristic for a certain set of hyperfine and quadrupole parameters of nearby magnetic nuclei, which are in turn very sensitive to the structural arrangement of these nuclei, as shown for a wide variety of biomolecules (Prisner et al. 2001).

The 2D-3-pulse ESEEM spectra of the minimal and ter-

tiary stabilized HHRz are shown in Figure 4. Both spectra display seven peaks that appear in both spectra at the same frequencies. The peak at about 4 MHz can be assigned in both cases to the free Lamor frequency of the sodium ions in the buffer based on field track experiments and previously reported data (Schiemann et al. 2003). The intensity of this peak scales with the concentration of the sodium ions. The peak at 1.3 MHz corresponds to the free Lamor frequency of $^{14}N$ nuclei that are farther away and not directly bound to the manganese center. This assignment is also supported by field track experiments. The four peaks at 0.7, 1.9, 2.5, and 4.9 MHz are assigned to a single nitrogen (nuclear spin $I[^{14}N] = 1$) coupled to the $^{55}Mn$ center, assuming that only the electronic $m_s = +\frac{1}{2} \leftrightarrow -\frac{1}{2}$ transition

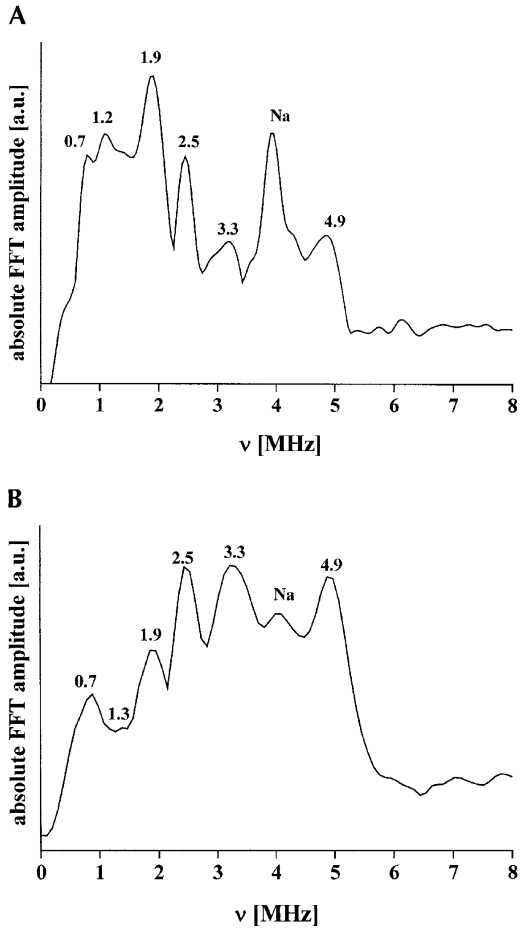


**FIGURE 4.** Skyline projection of a 2D-3-pulse ESEEM-spectrum of the mHHRz (*A*) and the tsHHRz (*B*). Both samples contained 0.2 mM ribozyme, 0.2 mM $Mn^{II}$, phosphate buffer, and 20% sucrose. The sample of the mHHRz contained 1 M NaCl while the sample of the tsHHRz contained 0.1 M. The experimental parameters for the 3-pulse sequence were as follows: T = 4.2 K, $\pi/2$-pulse length = 12 nsec, microwave attenuation = 12 dB using a 1-kW TWT, $\tau_{start}$ = 120 nsec, $T_{start}$ = 16 nsec, and $\tau$ and T were incremented in 8-nsec and 20-nsec steps, respectively. The dimensions of the array were 16 by 150 points for $\tau$ and T, respectively. $B_0$ was set to 3447 G. The shot repetition time was 20 msec (*A*) and 40 msec (*B*) and the number of shots per point was 50 in both cases.

contributes significantly to the spectrum (Benetis et al. 2002). The three peaks at 0.7, 1.9, and 2.5 MHz are the nuclear transitions $\nu_0$, $\nu_+$ and $\nu_-$ in the $m_S = -\frac{1}{2}$ electronic manifold of the single nitrogen nucleus and the peak at 4.9 MHz is the double quantum transition $\nu_{dq}$ in the $m_S = +\frac{1}{2}$ manifold of the same nucleus. The $\nu_0$ and $\nu_+$ transitions add up closely to the frequency of the double quantum transition $\nu_-$ in the same electronic manifold, as they should. This assignment is in agreement with the previously reported assignment for the mHHRz (Morrissey et al. 1999; Schiemann et al. 2003). An isotropic hyperfine coupling constant $A_{iso}$ of 2.3 MHz, a quadrupole coupling constant $\chi$ of 2.9 MHz, and an asymmetry parameter $\eta$ of 0.4 MHz can be calculated for the single nitrogen nucleus from the frequencies of these transitions, as explained in detail elsewhere (Morrisey et al. 1999). These parameters were in the case of the mHHRz used to determine the structure of the binding site (Schiemann et al. 2003).

In addition to the earlier reported spectra of the mHHRz, both spectra show one more peak at ~3.3 MHz, which may be assigned to a phosphorus ($I[^{31}P] = \frac{1}{2}$) possessing a hyperfine coupling of 5.4 MHz. A phosphorus nucleus with a hyperfine coupling smaller than the free Lamor frequency of $^{31}P = 6$ MHz gives a doublet centered around the free Lamor frequency and split by the hyperfine coupling. However, in many cases, as is true here, only the low frequency line can be observed (Flanagan and Singel 1987; Dikanov and Tsvetkov 1992). This phosphorous coupling does not originate from an interaction of the ribozyme-bound $Mn^{2+}$ with the phosphate buffer, since a measurement in Tris-buffer still shows this peak and it also does not originate from $Mn^{2+}$ free in solution interacting with the phosphate buffer, since a control sample of $Mn^{2+}$ in the same buffer but without the ribozyme shows no phosphate coupling. Instead the coupling is assigned to the phosphorous of the phosphate group bound to the manganese. This is supported by ENDOR experiments of Morrissey et al. on the mHHRz, who found a phosphorus hyperfine coupling of ~4 MHz (Morrissey et al. 2000) and by density functional theory (DFT) calculations (Schiemann et al. 2003).

Apart from the assignment it is obvious that the peaks in both spectra appear at the same frequencies, indicating that the structure of the high-affinity $Mn^{II}$ binding site is very similar in both ribozymes. It should, however, be noted that the intensity distribution of the peaks is different in both spectra. Several reasons could be responsible for that. One might be the different salt concentrations, which also lead to different relaxation times; another could be a slightly different structural arrangement.

In a second step the HYSCORE spectra in Figure 5 were acquired to further elucidate the similarity between both binding sites. On the diagonal both spectra exhibit peaks at 0.7, 1.9, 2.5, and 4.9 MHz. The peak at ~4 MHz on the diagonal of the mHHRz spectrum originates from the sodium ions, which is not present in the tsHHRz spectrum,

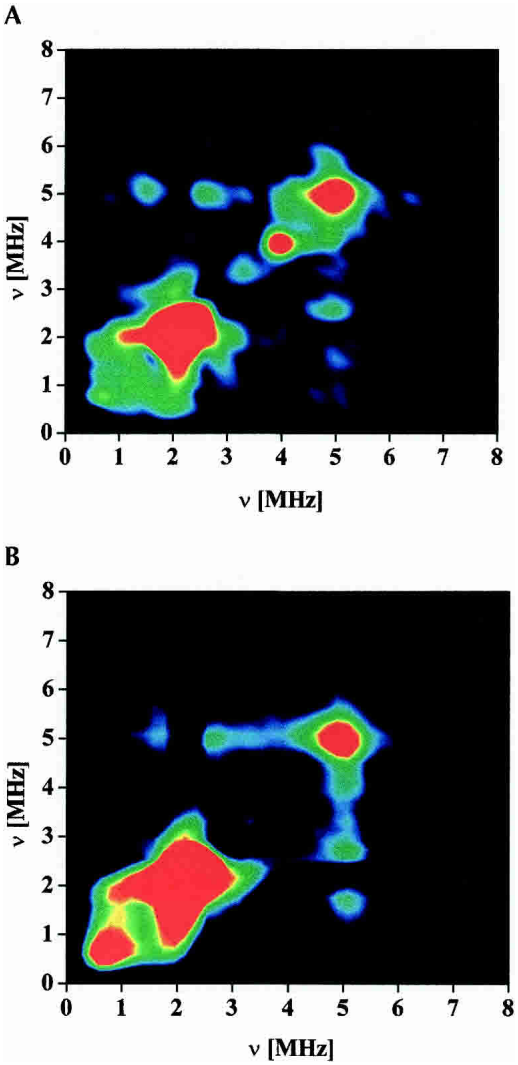


**FIGURE 5.** The (+,+) quadrants of the HYSCORE spectra of the high-affinity $Mn^{II}$ binding sites in the mHHRz (*A*) and the tsHHRz (*B*). The samples contained 0.2 mM ribozyme in phosphate buffer with 20% sucrose and 1 M NaCl (*A*) and 0.1 M NaCl (*B*). The parameters for the pulse sequence were as follows: T = 4.2 K, π/2-pulse-length = 12 nsec, π-pulse length = 24 nsec, microwave attenuation = 12 dB using a 1-kW TWT, τ = 136 nsec, $t_{1,strat}$ = 16 nsec, $t_{2,start}$ = 28 nsec, and $t_1$ and $t_2$ were incremented in 20-nsec steps. The dimensions of the array were 150 by 150 points for $t_1$ and $t_2$. $B_0$ was set to 3447 G. The shot repetition time was 20 msec (*A*) and 40 msec (*B*). The number of shots per point was 15 in both cases.

due to the smaller sodium ion concentration. In addition both spectra display the expected cross-correlation peaks at (2.5;4.9)/(4.9;2.5), (1.9;4.9)/(4.9;1.9), and (0.7;4.9)/(4.9;0.7). The cross-correlation peaks at (0.7;4.9)/(4.9;0.7) are weak in the case of the tsHHRz. Using longer pulses increases the intensity of these peaks but reduces the intensity of the others. Intensity between these peaks is due to the anisotropy of the couplings and peak shapes. The observation of all four cross-correlation peaks supports the assignment of the peaks to a single nitrogen nucleus. Furthermore, the similarity between both spectra underlines that both high-affinity binding sites are structurally very similar if not identical. This prompts the idea that the metal ion is bound at the same site in both ribozymes, which would be the G10.1 base of the sheared tandem base pair G · A, as has been proved by pulsed EPR studies in combination with density functional theory calculations (Schiemann et al. 2003) and site selective $^{15}$N-labeling (Vogt and DeRose 2003) for the mHHRz. This site was also found to be occupied in the crystal structure of the mHHRz (Pley et al. 1994; Scott et al. 1996). The final evidence that both binding sites are identical will be made by $^{15}$N-labeling of the G10.1 base in the tsHHRz.

Since the binding sites seem to be the same, one wonders why the manganese ion is so much more tightly bound in the tsHHRz. An answer could be based on the different dynamics of the two ribozymes. The tsHHRz is less flexible than the mHHRz due to the loop–loop interaction that holds stems I and II in more confined positions. Thus, the $Mn^{II}$ may be trapped in a conformation leading to the observed tight binding. The mHHRz, on the other hand, could be capable of adopting higher-energy conformations that are not accessible to the tsHHRz and that lead to a weakening or loosening of the $Mn^{II}$ binding. This difference in RNA dynamics is picked up by the cw EPR titrations since they were performed at room temperature in liquid solution. In contrast, the pulsed EPR measurements were done in the frozen state at 4.2 K where also the mHHRz has relaxed into the low-energy, tight-binding conformation.

Finally, it has been proposed that the metal ion bound at the conserved sheared G · A tandem base pair is directly involved in catalysis following a rather extensive structural rearrangement, since it is localized at ~20 Å from the cleavage site (Wang et al. 1999). However, the finding that the structure and site of the high-affinity $Mn^{2+}$ binding site seem to be the same in both ribozymes, whereas the catalytic activity of the tsHHRz is strongly enhanced, supports instead a role in folding and thus a structural role for this ion as previously suggested (Hammann and Lilley 2002). Thus, by stabilizing the RNA fold and forming a tighter binding site for the A9 metal ion, the loop–loop interactions enhance catalysis significantly even though the metal ion does not participate chemically in the catalytic reaction.

## MATERIALS AND METHODS

### Sample preparation

The ribozyme construct used is depicted in Figure 1. The substrate strand was protected against cleavage by incorporation of a methoxy group at the 2′-sugar site of the nucleotide C17. The RNA was obtained gel purified and desalted from Dharmacon. HPLC analysis showed that the strands were >95% pure. Autoclaved 0.1 M phosphate buffer solutions (pH = 7.0) containing 0.1 M or 1 M NaCl and 20% sucrose were added to yield final ribozyme concentrations of 0.2 mM for the pulsed EPR and 0.1 mM for the

titration experiments. The RNA concentrations were determined by UV-vis using the extinction coefficients given in Gray et al. (1995). For annealing the ribozyme to the noncleavable substrate, the following temperature program was run: 3 min at 90°C, 5 min at 60°C, 5 min at 50°C, 5 min at 40°C, and 15 min at 22°C. A sterilized buffer solution of $MnCl_2$ (Sigma) was subsequently added. Finally, the sample was heated again to 60°C and cooled on ice to form the tertiary structure. For the pulsed EPR measurements aliquots of 80 μL were transferred into sterilized EPR tubes. Neomycin B was purchased from Sigma and dissolved in sterilized phosphate buffer.

### cw EPR

cw X-band EPR spectra were recorded on a Bruker ESP300e EPR spectrometer, equipped with a rectangular $TE_{102}$ resonator. Titrations of the ribozyme with $Mn^{II}$ or neomycin B were performed at room temperature using a sterilized flat cell with a volume of 200 μL. The resulting $Mn^{II}$ EPR signals were base-line corrected and doubly integrated and the magnitude of the integral was plotted against the concentration of added $Mn^{II}$. Binding isotherms for $Mn^{II}$ were constructed and fitted according to Equation 1 by assuming cooperative binding of *n* sites (in the case of 1 M NaCl) or to Equation 2 by assuming *j* classes of *n* independent noninteracting binding sites (in the case of 0.1 M NaCl) to determine the dissociation constants $K_D$ (Horton et al. 1998; Schiemann et al. 2003).

cooperative binding
$$\frac{[Mn^{II}_{bound}]}{[HHRz]} = \frac{K_\pi [Mn^{II}_{free}]^n}{1 + K_\pi [Mn^{II}_{free}]^n} \quad (1)$$

with
$$K_\pi = \frac{1}{K_D^n}$$

non-interacting
$$\frac{[Mn^{II}_{bound}]}{[HHRz]} = \sum_{i=1}^{j} \frac{n_i [Mn^{II}_{free}]}{K_{D(i)} + [Mn^{II}_{free}]} \quad (2)$$

### Pulsed EPR

Pulsed EPR experiments were carried out on an ELEXSYS E580 pulsed X-band EPR spectrometer from Bruker using a FT-EPR probehead from Bruker and a cryostat for the temperature range from 4.2 K to 300 K from Oxford. Further technical specifications are described in Weber et al. (2002). The pulse sequences used were as described in Schiemann et al. (2003). An eight-step phase cycle was used to eliminate unwanted echoes. The acquired time spectra were treated in the following way: the decay was fitted exponentially and subtracted, the resulting spectrum multiplied with a Hamming window function, zero-filling applied, and the time traces Fourier transformed. The differences between the HYSCORE and ESEEM spectra reported previously and those shown here, are attributed to the presence of sucrose, which leads to a more homogeneous glass and better spectra.

## ACKNOWLEDGMENTS

The financial support of the DFG is gratefully acknowledged (SFB 579) and T.F. Prisner is thanked for his support. S. Lyubenova is thanked for technical support and discussions.

*Received July 19, 2004; accepted November 2, 2004.*

## REFERENCES

Benetis, N.P., Dave, P.C., and Goldfarb, D. 2002. Characteristics of ESEEM and HYSCORE spectra of S > ½ centers in orientationally disordered systems. *J. Magn. Reson.* **158:** 126–142.

De la Pena, M., Gago, S., and Flores, R. 2003. Peripheral regions of natural hammerhead ribozymes greatly increase their self-cleavage activity. *EMBO J.* **22:** 5561–5570.

Dikanov, S.A. and Tsvetkov, Y.D. 1992. *Electron spin echo envelope modulation (ESEEM) spectroscopy*. CRC Press, Boca Raton, FL.

Feig, A.L. 2000. In *Metal Ions in biological systems* (eds. A. Siegel and H. Siegel), Vol. 37, pp. 157–177. Marcell Dekker, New York.

Flanagan, H.L and Singel, D.J. 1987. Analysis of $^{14}N$ ESEEM patterns of randomly oriented solids. *J. Chem. Phys.* **87:** 5606–5616.

Gesteland, R.F., Cech, T.R., and Atkins, J.F. 1999. *The RNA world*. Cold Spring Harbor Laboratory Press, Cold Spring Harbor, NY.

Gray, D.M., Hung, S.H., and Johnson, K.H. 1995. Absorption and circular dichroism spectroscopy of nucleic acid duplexes and triplexes. *Methods Enzymol.* **246:** 19–34.

Hammann, C. and Lilley, D.M.J. 2002. Folding and activity of the hammerhead ribozyme. *Chembiochem.* **3:** 690–700.

Hermann, T. and Westhof, E. 1998. Aminoglycoside binding to the hammerhead ribozyme: A general model for the interaction of cationic antibiotics with RNA. *J. Mol. Biol.* **276:** 903–912.

Horton, T.E., Clardy, D.R., and DeRose, V.J. 1998. Electron paramagnetic resonance spectroscopic measurement of $Mn^{2+}$ binding affinities to the hammerhead ribozyme and correlation with cleavage activity. *Biochemistry* **37:** 18094–18101.

Khvorova, A., Lescoute, A., Westhof, E., and Jayasena, S.D. 2003. Sequence elements outside the hammerhead ribozyme catalytic core enable intracellular activity. *Nat. Struct. Biol.* **10:** 708–712.

Misra, S.K. 1996. Interpretation of $Mn^{2+}$ EPR spectra in disordered materials. *Appl. Magn. Reson.* **10:** 193–216.

Morrissey, S.R., Horton, T.E., Grant, C.V. Hoogstraten, C.G., Britt, R.D., and DeRose, V.J. 1999. $Mn^{2+}$-nitrogen interactions in RNA probed by electron spin-echo envelope modulation spectroscopy: Application to the hammerhead ribozyme. *J. Am. Chem. Soc.* **121:** 9215–9218.

Morrissey, S.R., Horton, T.E., and DeRose, V.J. 2000. $Mn^{2+}$ sites in the hammerhead ribozyme investigated by EPR and continuous-wave Q-band ENDOR spectroscopies. *J. Am. Chem. Soc.* **122:** 3473–3481.

Penedo, J.C., Wilson, T.J., Jayasena, S.D., Khvorova, A., and Lilley, D.M.J. 2004. Folding of the natural hammerhead ribozyme is enhanced by interaction of auxiliary elements. *RNA* **10:** 880–888.

Pley, H.W., Flaherty, K.M., and MacKay, D.B. 1994. Three-dimensional structure of a hammerhead ribozyme. *Nature* **372:** 68–74.

Prisner, T.F., Rohrer, M., and MacMillan, F. 2001. Pulsed EPR spectroscopy: Biological applications. *Annu. Rev. Phys. Chem.* **52:** 279–313.

Schiemann, O., Fritscher, J., Kisseleva, N., Sigurdsson, S.T., and Prisner, T.F. 2003. Structural investigation of a high-affinity $Mn^{II}$ binding site in the hammerhead ribozyme by EPR spectroscopy and DFT calculations. Effects of neomycin B on metal-Ion binding. *Chembiochem.* **4:** 1057–1065.

Schiemann, O., Piton, N., Mu, Y., Stock, G., Engels, J.W., and Prisner, T.F. 2004. A PELDOR-based nanometer distance ruler for oligonucleotides. *J. Am. Chem. Soc.* **126:** 5722–5729.

Scott, W.G., Murray, J.B., Arnold, J.R.P., Stoddard, B.L., and Klug, A. 1996. Capturing the structure of a catalytic RNA intermediate: The hammerhead ribozyme. *Science* **274:** 2065–2069.

Vogt, M. and DeRose, V.J. 2003. $Mn^{2+}$ sites investigated by advanced EPR techniques: In depth study of $Mn^{2+}$ ion-binding sites in the hammerhead ribozyme. *ACS Symp. Ser.* **858:** 193–211.

Wang, S., Karbstein, K., Peracchi, A., Beigelman, L., and Herschlag, D. 1999. Identification of the hammerhead ribozyme metal ion binding site responsible for rescue of the deleterious effect of a cleavage site phosphorothioate. *Biochemistry* **38:** 14363–14378.

Weber, A., Schiemann, O., Bode, B., and Prisner, T.F. 2002. PELDOR at S- and X-band frequencies and the separation of exchange coupling from dipolar coupling. *J. Magn. Reson.* **157:** 277–285.